Method of Designing High-Speed Generators for the Biogas Plant

Aynur Yakupov‡, Flur Ismagilov*, Irek Khayrullin*, Viacheslav Vavilov*

*Department of Electromechanics, Ufa State Aviation Technical University, Ufa, Russian Federation

(aynurpov@mail.ru, ismagilov137@gmail.com, irekkhayrullin@yandex.com, s2_88@mail.ru)

‡ Corresponding Author: Yakupov Aynur Mahmutovich, Tel- +79272349921, e-mail: aynurpov@mail.ru

Received: 02.02.2016 Accepted:07.05.2016

Abstract- One of the prospects for further development of gas turbine engines application in the decentralized energy system is the usage of microturbine units operating on biofuel. In this paper, a new method of microturbines designing is proposed, also some aspects and special features in the designing of micro-turbines are considered. Computerized modelling also was made by authors to test the method on developing the high speed generator for biofuel microturbine. In paper authors made the experiment to check the computer modelling and it is showed that method of designing allow to develop the generator with the needed accuracy.

Keywords- Microturbines, High-Coercivity permanent magnets, High speed generator, Biofuel

1. Introduction

One of the prospects for further development of gas turbine engines application in the decentralized energy system is the usage of microturbine units (MTU). The following features can be referred to the advantages of MTU: a minimum amount of moving parts (in modern MTU configurations a turbine, compressor and electric generator are located on the same shaft); the possibility of cogeneration and trigeneration; flexibility in the usage of fuel (MTU can efficiently work both on traditional fuels like natural gas, LPG, diesel fuel, kerosene, and on the low-calorie and sour gases, such as associated gas, coal mine gas and biogas). Furthermore, MTU has high efficiency coefficient (efficiency in cogeneration mode can reach 92%) [1, 2, 3].

The effectiveness of MTU is determined not only by the efficiency of its gas turbine engine, but also by the efficiency of its electrical energy production part - electric generator. As we can see in the constructive schemes of MTU of world leaders in microturbine technologies (Capstone, Elliot, TurbecS.p.A) an electric generator is located on the same shaft with a turbine and constitutes a high speed generator (HSG) (48 000 - 96 000 rpm) with high-coercivity permanent magnets (HCPM), Fig. 1. In this case, an important task for improving the economic viability of MTU is to develop new approaches and design methodologies of HSG, which will give an opportunity to improve the accuracy of design calculations and to minimize project costs.

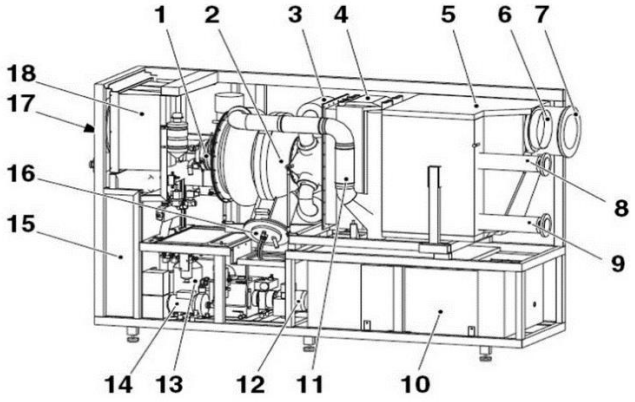

Fig.1. Microturbine installation Turbec T 100 [3]

1- HSG; 2-turbine; 3- pipe from the recuperator; 4- recuperator; 5- heat exchanger; 6- output of air ventilation; 7- exhaust pipe; 8- water inlet pipe to the heat exchanger; 9- hot water pipe to the consumer; 10- power electronics; 11 - pipe to recuperator; 12 - oil pump; 13- exhaust air pump; 14- cooling water pump; 15- control system; 16- combustion chamber; 17- input for air; 18- air filter.

2. Problem

In well-known approaches to the designing of electromechanical energy converters (EMEC) there is a certain sequence of calculations, which is also used in designing of HSG. This sequence is based on electromagnetic calculations, results of which determine the size of EMEC active elements [4, 5] and the electromagnetic loads of EMEC magnetic circuit. Thereafter thermal and mechanical calculations are made and the obtained amounts are adjusted on the basis of these calculations results.

In papers [6-17] designing methods of the high-speed generators for biogas units are described. Moreover, in these

papers the following design consequence is used: firstly, generator electromagnetic parameters are calculated, then thermal ones come and, in the end, mechanical parameters follow them. This does not allow taking into account interaction between thermal and electromagnetic processes or electromagnetic and mechanical ones, which leads to significant design error. For example, in paper [6] losses are calculated first, then the generator thermal condition is rated. Although it is known that the generator thermal condition influences the losses. Therefore, the calculations must be done in combination; or adjustment of the electromagnetic calculations must be done after the thermal ones. In papers [7], [8] the designing method of the high-speed generator for flywheel applications in software package Ansoft Maxwell is presented. In this work the thermal action is taken into account but the analytical procedure is not given, although the analytical calculations are important for doing such kind of designing work. In papers [9-11] the analytical calculations of the high-speed generator for Renewable Energy Applications are presented. However, the action of temperature on permanent magnets parameters is not considered, furthermore, the mechanical calculations that must be done together with the electromagnetic calculations are slightly involved. In papers [12–14] the high-speed generator designed by ABB for microturbine units is described. The capacity of such generator is 100 kWt at rotor speed of 70000 rpm. Although the procedure for the generator calculation is not given in these papers. In paper [15] the electromagnetic calculations of high-speed generators are described but herewith the action of temperature on the electromagnetic processes is considered. In paper [16] the analytical procedure for high-speed generator torque calculation is presented. In paper [17] interactions between the temperatures, mechanical performance and electromagnetic processes are not taken into account at designing the high-speed generators for alternative energetics.

Therefore, the purpose of this paper is to develop the analytical procedure for designing the high-speed generator for alternative energetics. This procedure includes interaction of the mechanical performance, thermal and electromagnetic processes. Designing the high-speed generator with improved parameters and conducting its experimental investigations are the second purpose. The generator ABB presented in paper [13] is taken as an analogue for comparison.

The novelty of the paper is as follows: combination of the thermal, mechanical and electromagnetic calculations is supposed using at designing the high-speed generator. In this case the thermal, mechanical and electromagnetic calculations are done in combination and as a result we get the high-speed generator designed with required power, including all operating parameters. Moreover, it is important to note that, unlike the existing approaches to designing the high-speed generator with high-coercivity permanent magnets, the magnetic circuit calculation must be done at the idle mode. As at the load mode the armature reaction magnetic field decreases the magnetic density value in the air gap created by HCPM. Therefore, it is necessary to check the magnetic field saturation of the HSG with HCPM at the idle mode.

3. Methodology of MTU Designing

NdFeB alloy is taken as a material of the rotor with HCPM, since it outperforms, and has a lower cost and simpler production technology compared to other types of HCPM (for example, SmCo alloy).

At design calculations the rotor speed, rated voltage and wattage of HSG with HCPM, type and size of the network load, as well as the properties of HCPM (residual induction and coercive force) are considered to be supplied. Also it is necessary to know parameters of the cooling system of the HSG with HCPM, type of refrigerant, its temperature and pressure at the cooling system inlet.

The main requirement for the designing is to determine geometric parameters of the HSG with HCPM, electromagnetic and thermal loads, the HSG mass properties as well.

The maximum possible diameter of HSG rotor in the case of mechanical strength [18] was determined:

$$D_1 = \frac{n}{c_1\sqrt{\frac{\sigma g}{\rho k_a}}}, \quad (1)$$

where g is acceleration of gravity; σ is HCPM yield strength; γ is density of HCPM material; c_1 is estimated coefficient $\left(c_1 = \frac{60}{\pi}\right)$; k_a is safety factor for the yield strength; n is HSG rotor speed .

The maximum diameter of the rotor back and the minimum possible thickness of HCPM are also defined by the same formula. Also it is necessary to take into account the rotor material tensile strength and density of the rotor material.

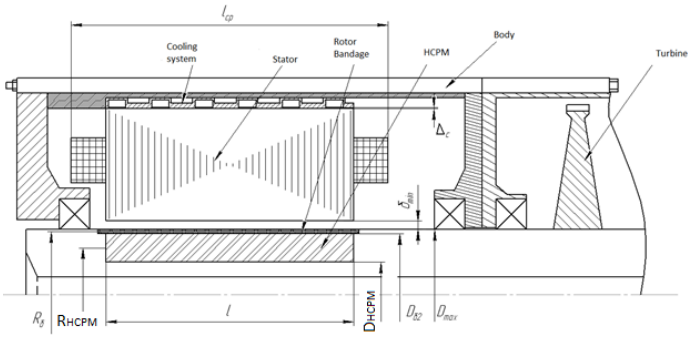

Fig. 2. Calculation drawing of the HSG with HCPM in the MTU

As the output power is determined by the volume of HCPM, which depends on the effective length and thickness of HCPM, therefore, the HCPM thickness can be assumed as predetermined, thus varying its length. Accordingly to that, the thickness of the rotor shroud shell, Fig. 2, is defined as [19]:

$$\delta_б = \frac{\Omega^2\left[\rho_б R_б\left(D_{б1}^2 + D_{б2}^2\right) + \rho_{\text{HCPM}} R_{\text{HCPM}}\left(D_{\text{HCPM1}}^2 + D_{\text{HCPM2}}^2\right)\right]}{8\sigma} \quad (2)$$

where $\delta_б$ is the thickness of the rotor shroud shell; Ω is the HSG angular velocity, rad / s; $\rho_б$, ρ_{HCPM} are density of the shroud material and the HCPM material, respectively; σ is tensile strength to the yield of shroud shell material; $R_б$, $D_{б1}$, $D_{б2}$, R_{HCPM}, D_{HCPM1}, D_{HCPM2} are geometric parameters of the HSG.

Geometric parameters are determined according to the Fig. 2:

$$D_{б1} = D_{\max},$$
$$D_{б2} = D_{\max} - 2\delta_б,$$
$$D_{НСРМ1} = D_{б2},$$
$$D_{НСРМ2} = D_{НСРМ1} - 2h_М,$$
$$R_б = \frac{D_{\max} - \delta_б}{2},$$
$$R_{НСРМ} = \frac{D_{\max} - 2\delta_б - h_М}{2}.$$

By taking into account geometrical ratios and skipping intermediate mathematical calculations, (2) can be represented as:

$$\rho_б\delta_б^3 - \delta_б^2\left[\rho_б D_{\max} - 4\rho_{НСРМ}h_М + \rho_б\right] + \\ +\delta_б\left[\rho_б D_{\max} - 4\rho_{НСРМ}D_{\max}h_М + 4\rho_{НСРМ}h_М^2 - \frac{8\sigma}{\Omega^2}\right] + \\ +\rho_{НСРМ}D_{\max}^2 h_М - 2\rho_{НСРМ}D_{\max}h_М^2 + \rho_{НСРМ}h_М^3 = 0 \quad (3)$$

Expression (3) is a cubic equation, which solution can be found using trigonometric Vieta`s formula. To do this, (3) can be rewritten as:

$$\delta_б^3 - a\delta_б^2 + b\delta_б + c = 0, \quad (4)$$

Where

$$a = \frac{\left[\rho_б D_{\max} - 4\rho_{НСРМ}h_М + \rho_б\right]}{\rho_б};$$
$$b = \frac{\left[\rho_б D_{\max} - 4\rho_{НСРМ}D_{\max}h_М + 4\rho_{НСРМ}h_М^2 - \frac{8\sigma}{\Omega^2}\right]}{\rho_б};$$
$$c = \frac{\rho_{НСРМ}D_{\max}^2 h_М - 2\rho_{НСРМ}D_{\max}h_М^2 + \rho_{НСРМ}h_М^3}{\rho_б}$$

are coefficients of the cubic equation. Then:

$$Q_1 = \frac{a^2 - 3b}{9};\ Q_2 = \frac{2a^3 - 9ab + 27}{c};\ Q_3 = Q_1^3 - Q_2^2;\ \varphi = \frac{1}{3}\arccos\left(\frac{Q_2}{\sqrt{Q_1^3}}\right)$$

The magnitude of the thickness of the shell is determined by the binding based on the values Q_1 and Q_3: if $Q_3 > 0$, then (3) has three real roots, which are defined as:

$$\delta_{б1} = -2\sqrt{Q_1}\cos(\varphi) - \frac{a}{3}, \quad (5)$$

$$\delta_{б2} = -2\sqrt{Q_1}\cos\left(\varphi + \frac{2}{3}\pi\right) - \frac{a}{3}, \quad (6)$$

$$\delta_{б1} = -2\sqrt{Q_1}\cos\left(\varphi - \frac{2}{3}\pi\right) - \frac{a}{3}. \quad (7)$$

Of the three measured values the maximum one is chosen. If $Q_3 < 0$ and $Q_1 > 0$, then (3) has one real root:

$$\delta_{б1} = -2\,\mathrm{sgn}(Q_2)\sqrt{Q_1}\,\mathrm{ch}(\varphi) - \frac{a}{3}. \quad (8)$$

If $Q_3 < 0$ and $Q_1 < 0$ then (3) has one real root:

$$\delta_{б1} = -2\,\mathrm{sgn}(Q_2)\sqrt{|Q_1|}\,\mathrm{sh}(\varphi) - \frac{a}{3}. \quad (9)$$

If $Q_1 = 0$ then (3) has one real root:

$$\delta_{б1} = \sqrt[3]{c - \frac{a^3}{27}} - \frac{a}{3}. \quad (10)$$

If $Q_1 = 0$ then (3) has one real root:

$$\delta_{б1} = -2\sqrt[3]{Q_2} - \frac{a}{3}, \quad (11)$$

$$\delta_{б2} = \sqrt[3]{Q_2} - \frac{a}{3}. \quad (12)$$

Thus, initially, on the basis of mechanical strength conditions, the shroud thickness and maximum possible rotor diameter are defined.

Pole overlap ratio is set [20], and a number of geometric parameters for the HSG are determined:

$$D_{ст} = D_{\max} + 2\delta_{\min} + \delta_б, \quad (13)$$

where $\delta_{\min}$ is the minimum air gap selected from technological considerations, taking into account thermal and mechanical expansions of the rotor shell shroud while in operation. Whereas, neglect of the thermal and mechanical expansions can lead to excessive swelling of the binding membrane and wedging of the rotor in the stator. Engineering calculations performed by the authors have shown that for the HSG with rotor speed of 60,000 rpm and a rotor diameter of 60 mm made from titanium or carbon-fiber the bandage thickness $\delta_{\min}$ must be 1 – 1.2 mm.

Further, a number of geometric dimensions of the magnetic circuit for the HSG with HCPM and induction in the air gap at an idle mode, without thermal demagnetization of permanent magnets can be found:

$$b_m = D_{\max}\sin\frac{\pi\alpha_i}{2p}, \quad (14)$$

$$\tau = \frac{\pi D_{\max}}{2p}. \quad (15)$$

$$\tau_{ст} = \frac{\pi D_{ст}}{2pmq}, \quad (16)$$

$$B_\delta = \frac{b_m B_r}{k_p + \frac{\delta B_r k_\delta}{\mu_0 H_c h_М}}, \quad (17)$$

where τ is the pole pitch of the rotor; α_i is the coefficient of HSG rotor pole overlapping; p is a number of HSG rotor pole pairs; Dст is the diameter of the stator bore; m is a number of phases; $\tau_{ст}$ is the stator pole pitch; q is a number of slots per pole and phase; k_δ is the Carter Coefficient; μ_0 is the vacuum

permeability; k_p is the scattering coefficient of the magnetic rotor system with HCPM.

After that, the magnetic material of the stator by reference to the magnitude of idling induction (maximal induction value in the HSG air gap) is defined, and the magnetic circuit is calculated by standard methods.

Having defined the bandage thickness and after the calculation of the magnetic circuit at a maximum induction it is needed to set the maximum steady-state temperature of permanent magnets. Basing on the maximum HCPM steady-state temperature, the induction in the HSG air gap at an operation mode and the temperature in the HSG gap are found [21]:

$$B_r(\Theta) = B_r\left(1-\frac{k_{Br}(\Theta_{HCPM}-23)}{100}\right), \quad (18)$$

$$H_c(\Theta) = H_c\left(1-\frac{k_{Hc}(\Theta_{HCPM}-23)}{100}\right), \quad (19)$$

$$B_\delta = \frac{b_m B_r(\Theta_{HCPM})}{k_p + \frac{\delta B_r(\Theta_{HCPM})k_\delta}{\mu_0 H_c(\Theta_{HCPM})h_M}}, \quad (20)$$

where $B_r(\Theta),\ H_C(\Theta)$ are the current values of residual induction and coercive force of HCPM, respectively; B_r, H_C are the values of residual induction and coercive force of HCPM specified in the technical data, respectively; Θ_{HCPM} is the temperature of HCPM; k_{Br} is the temperature coefficient of HCPM residual induction; k_{Hc} is the temperature coefficient of HCPM coercive force.

The magnitude of the magnetic induction in the air gap of HSG with HCPM is affected not only by the temperature of HCPM, but also by the demagnetizing effect of armature reaction, which is determined by the inductive reactance in the longitudinal and transverse axes and a design scheme of the HSG magnetic rotor system In this case, if to determine the percentage, for which the induction in the air gap due to the effect of armature reaction field can be reduced, it is possible to calculate the inductances that reduce the induction in the air gap up to the predetermined parameter and a number of turns in the stator winding using the present proportions. To do this, in the methodology of the HSG with HCPM designing it is proposed to introduce the coefficient which takes into account the reduction of magnetic induction in the air gap under the armature reaction field (k_{ra}):

$$w = \frac{U_\phi}{4k_{ph}k_w f k_{ra} B_\delta l \tau}, \quad (21)$$

$$x_{ad} = \frac{\sqrt{2}\mu_0 \tau k_w 2wPZ_{\text{nom}}}{\pi k_\delta k_{\mu d}\delta U_{ph}\cos\varphi D_{\text{ст}} B_\delta k_{ra} a} k_{ad}, \quad (22)$$

$$x_{aq} = \frac{\sqrt{2}\mu_0 \tau k_w 2wPZ_{\text{nom}}}{\pi k_\delta k_{\mu q}\delta U_{ph}\cos\varphi D_{\text{ст}} B_\delta k_{pa} a} k_{aq}. \quad (23)$$

where Z_{nom} is load resistance of the HSG with HCPM; P is HSG active power; $k_{\mu q}$, $k_{\mu d}$ are saturation coefficients for the longitudinal and transverse axes determined by calculation of the magnetic circuit; k_{ad}, k_{aq} are coefficients of longitudinal and transverse fields of the armature reaction; a is a number of parallel branches of the stator winding.

It is important to note that for the correct defining of the saturation coefficients in the longitudinal and transverse axes after determining the magnetic flux density in the air gap according to the temperature conditions and taking into account the coefficient of armature reaction, re-calculation of the magnetic circuit should be done. Its task is not to check magnetic stator saturation capacity, but to define electromagnetic loads of the HSG at a nominal mode.

Like in the well-known techniques, the current density in the HSG windings [22] is predefined, and its value is determined by the area occupied by a winding in the slot, the coil end length and coil resistance. Thermal circuit of the HSG was developed. It helps to determine the total loss [23, 24] allocated by a cooling system.

Common type of a coolant, its temperature and cooling system inlet pressure are given in design specifications. Taking the given parameters, using Newton`s formula and varying jacket wall thickness, the temperature of cooling jacket inner wall can be found by the following way:

$$\Theta_{\text{po}} = \frac{\sum P_{en}}{\lambda\left[2\pi\left(D_{\text{ст}} + 2h_p + 2h_c + 2\Delta_c\right) + 2l\right]} + \Theta_T, \quad (24)$$

where λ is coefficient of heat transfer from the cooling jacket to the coolant; Θ_{po} is wall temperature of the HSG cooling jacket; Θ_T is temperature of the coolant; $\sum P_{en}$ is total losses in the HSG; h_p is groove height; Δ_c is wall thickness of the HSG cooling jacket.

If the temperature of the cooling jacket and the temperature in the air gap zone are known, so tooth zone temperature and groove surface temperature can be determined. Then it is necessary to do a revised calculation of the current density in the windings. The equation of heat conduction for the winding is written as follows:

$$I^2 r dt = c_x G_w d\Theta + 2\lambda_p h_p \Theta_z + \lambda_c b_p \Theta_c + \lambda_\delta b_{z\min}\Theta_\delta \quad (25)$$

where r is active resistance of the HSG winding with HCPM; c_x is copper specific heat; G_w is winding mass; Θ_z, Θ_c, Θ_δ are teeth temperature, back temperature and air gap temperature of the HSG, respectively; $\lambda_p, \lambda_c, \lambda_\delta$ are coefficients of heat transfer from the winding to the teeth, and to the back and to the air gap, respectively.

Taking into account that the resistance $r = \frac{\gamma l_{\text{cp}}}{S_w}$ (where γ is the winding specific electric resistance), the winding mass $G_w = \rho_{\text{cu}} l_{cp} S_w$ and the winding area $S_w = \frac{I}{j_{\max}}$, while skipping the intermediate mathematical calculations the

following formula is obtained:

$$\left(j_{\max}{}^2 l_{cp}\gamma\text{-}2\lambda_p h_p \Theta_z \frac{j_{\max}}{I} - \lambda_c b_p \Theta_c \frac{j_{\max}}{I} - \lambda_\delta b_{z\min} \Theta_\delta \frac{j_{\max}}{I} \right) dt = c\rho_{cu} l_{av} d\Theta \quad (26)$$

Having integrated (26), the adjusted value of current density for the given and calculated temperatures of the HSG active parts is determined. The resulting value is compared with the accepted one and if the difference between them is more than 10% I is necessary to make corrections in the nominal winding area. Moreover, (26) can be used in calculations of HSG transfer modes.

4. Computerized Modeling

To give the developed procedure adequate assessment the authors have made calculations of the major dimensions of the HSG with capacity of 120 kWt and revolution rate of 50000 rpm. The calculated dimensions are given in Table 1.

Using the obtained dimension data the finite-element model was designed in Ansoft Maxwell software package. As the result of the modeling we get the flux density distribution spectrum in the HSG active parts at different angles of rotor rotation (Fig.3, Fig.4), and the HSG magnetic field pattern (Fig. 5) as well.

Table 1. The geometric dimensions of the HSG calculated by the supposed procedure

Dimension	Value
Effective length, mm	150
Rotor magnets diameter, mm	60
Stator bore diameter, mm	74
Stator OD, mm	150
Permanent magnets type	Sm2Co17
Core steel grade	Siliceous steel 2421
Shaft	Fe
Rotor bandage	Titanium

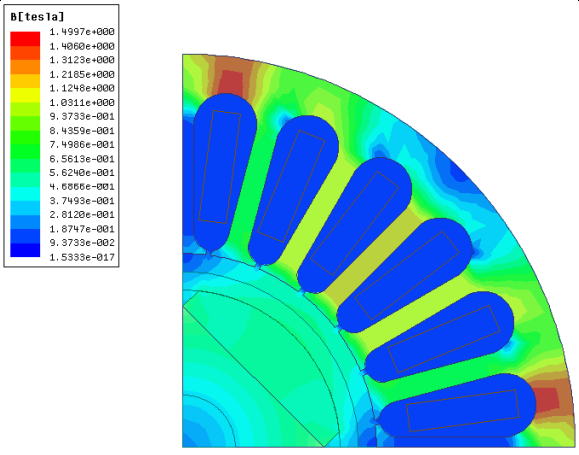

Fig. 3. Flux density distribution spectrum over a cross section of the HSG stator at the zero position

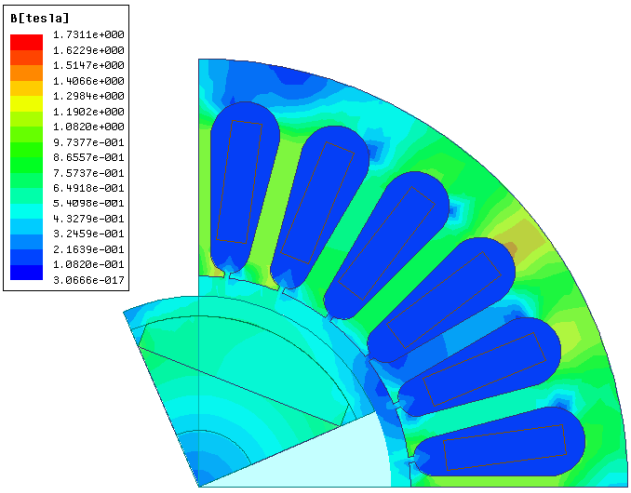

Fig. 4. Flux density distribution spectrum over a cross section of the HSG stator at the rotor rotational angle of 23 degrees

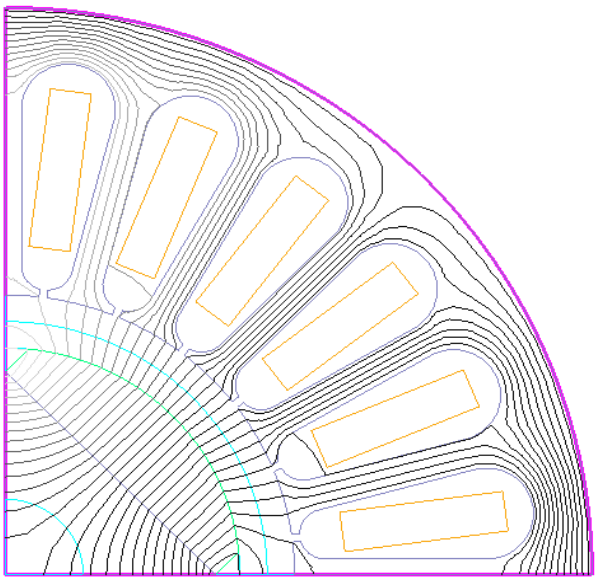

Fig. 5. Pattern of the magnetic field distribution in the HSG

Furthermore, oscillograms of currents and voltages (Fig. 6, Fig.7) were obtained, and a curve of the flux density distribution in the generator air gap (Fig.8) was plotted as the result of the computerized modeling.

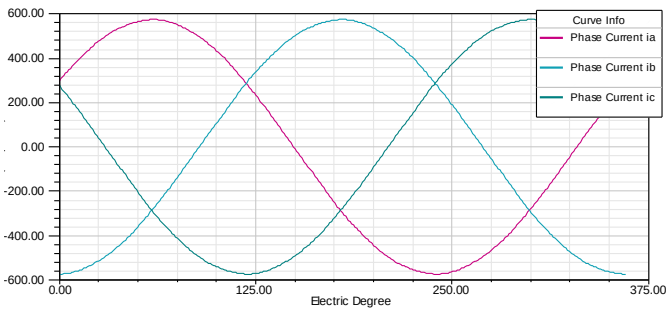

Fig. 6. Currents oscillograms

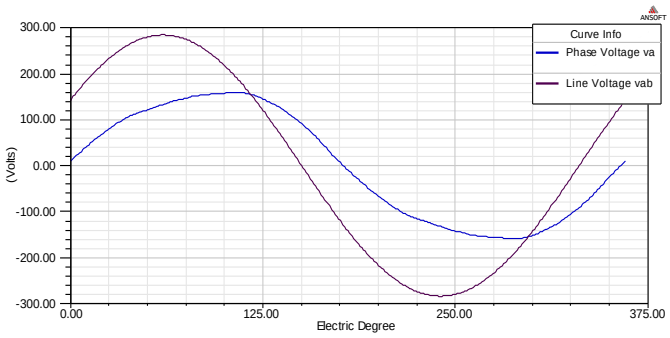

Fig. 7. Voltages oscillograms

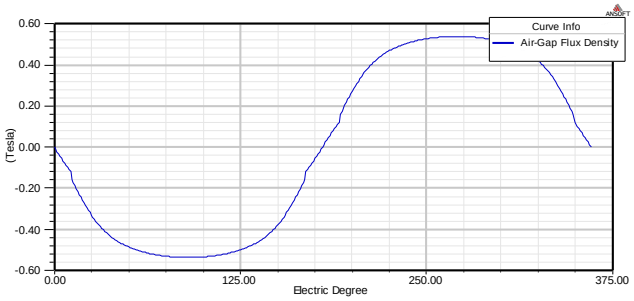

Fig. 8. Magnetic field distribution in the generator air gap

The results of the conducted computerized modeling show that the developed procedure is of high accuracy, as the results mentioned above have complete convergence to the results obtained from the analytical calculations. Schematic drawings for making the experimental model were developed according to the computerized modeling results.

5. Experiment

The proposed method has been tested while producing the HSG with HCPM for the MTU 120 kW with rotor speed of 60,000 rpm (Fig. 9) at the Department of Electromechanics VPO "USATU" and it has been proved to be effective.

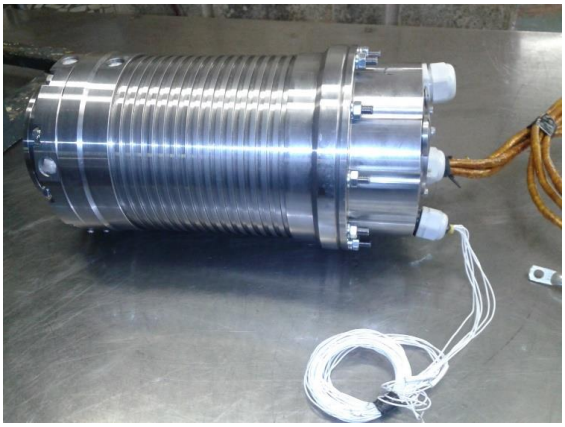

Fig. 9. Contactless magneto generator (with the power of 120 kW and rotor speed of 60,000 rpm)

Characteristics and main dimensions of the designed generator and the production generator installed in the microturbine unit Turbec T100 are shown in Table2.

As it is seen from Table 2 the generator designed according to the suggested procedure has larger capacity at less weight-size parameters and rotor speed.

In Fig. 10 the stator magnetic circuit of the designed generator is shown. Testing of the designed generator was conducted on the specialized facility, Fig. 10. The rotor drawing is in Fig. 11.

Electrical load from the model was transmitted to effective resistance of the boot block at a pitch of ΔN =5kWt with total range of Nmax =100 kWt.

Together with the test generator (designed and developed according to the suggested procedure) the production generator Turbec T100 (Generator Turbec T100) was being tested.

Table 2. Main geometrical parameters of the designed generator (generator USATU) and the production generator installed in the microturbine unit Turbec T100 (Generator Turbec T100)

Rated characteristics	Generator USATU	Generator Tubec T100
Rated revolutions, rpm	50000	70000
Rated output voltage, V	115/200	220/400
Stator diameter, mm	137	137
Stator length, mm	180	180
Rotor HCPM diameter, mm	59	59
Generator weight, kg	32	40

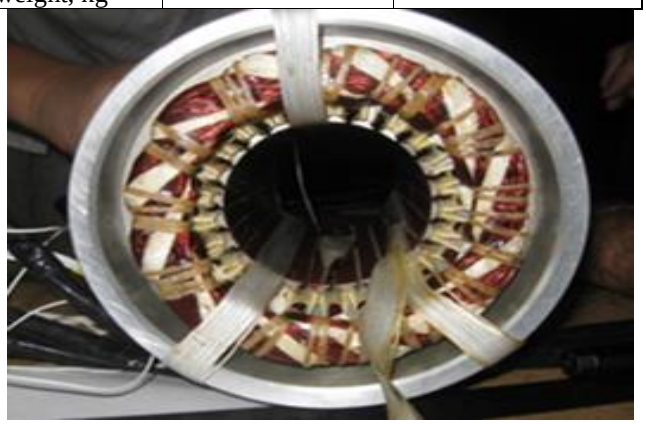

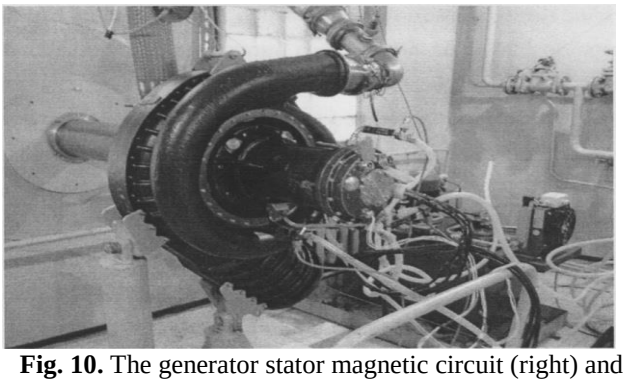

Fig. 10. The generator stator magnetic circuit (right) and Test facility (left)

As there was no cooling system in the test facility the tests were run not at full capacity, but only at load (resistance) of 20 Ohm for each phase at the rotor speed of up to 50000 rpm and ambient temperature of not less than 10◦C. During the experimental research different variants of both machines were considered. They are Stator USATU-rotor Turbec, Stator Turbec-rotor USATU, stator and rotor USATU, stator and rotor Turbec. The results of the Experimental research are shown in Fig. 12.

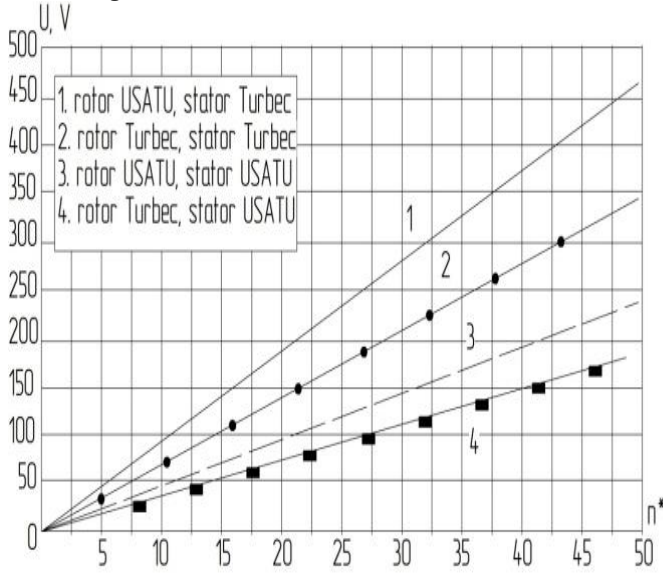

Fig.12. The experimental research results

From the results of the experimental research it is seen that the rotor designed according to the supposed procedure (rotor USATU) provides the capacity of 33135 Wt at the resistance of 20 Ohm, while the production generator rotor Turbec T100 gives capacity of 17340 Wt, i.e. the developed generator has higher power performance at lower weight-size parameters. It proves the effectiveness of the supposed procedure

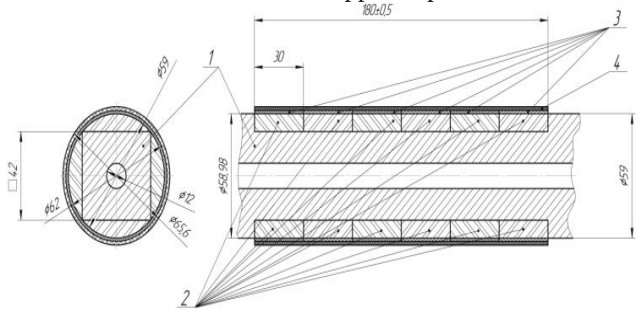

Fig. 11. Schematic drawing of the generator rotor

6. . Conclusion

Thus, in this paper the methodology of designing high-speed generator with HCPM with regard to their thermal and mechanical loads is presented. It is shown that the calculation of the magnetic circuit and checking it for saturation for HSG with HCPM must be conducted at an idling mode. Also using Vieta`s formula the technique of determining the thickness of the high electromechanical energy converters shell bandage is represented, and it allows to determine rotor shroud thickness and the value of the minimum air gap at minimal initial conditions with sufficient accuracy.

The results obtained can be used in practice in the development of non-contact high-speed magneto generators for microturbine systems in biofuel plants.

The research is carried out under the grant from Russian Science Foundation (project №16-19-10005).

References

[1] Microturbine install Capstone // Electronic resource URL: http: //www.bpcenergy.ru/imgcompany/bpcenergy/events/2009/Capstone_broshure5.pdf (reference date 02/22/2015)

[2] Portable Biogas Microturbine Power System Installation // Electronic resource http://web.ornl.gov/sci/de_materials/documents/CETC_MTrailer.pdf (reference date 02/22/2015)

[3] Gas microturbines Turbec T100 series // Electronic resource URL: http://www.powercity.ru/site/ru/catalog/46.html (reference date 02/22/2015)

[4] Front Cover. K. G. Upadhyay Design of Electrical Machines.. New Age International, 2011 - Electric machinery - 440 pages.

[5] Hendershot J.R., Miller T.J., "Design of brushless permanent-magnet motors // Oxford University Press, 1996.

[6] Co Huynh, Liping Zheng, Dipjyoti Acharya. Losses in High Speed Permanent Magnet Machines Used in Microturbine Applications // Journal of Engineering for Gas Turbines and Power. – March 2009. – Vol. 131.

[7] Nagorny A., Dravid N., Jansen R., Kenny B. Design Aspects of a High Speed Permanent Magnet Synchronous Motor/Generator for Flywheel Applications // NASA/TM–2005–213651.-2005.-pp.1-7

[8] A.S. Nagorny, R.H. Jansen, D.M. Kankam, Experimental performance evaluation of a highspeed permanent magnet synchronous motor and drive for a flywheel application at different frequencies, in Proceedings of 17th International Conference on Electrical Machines—ICEM, 2006

[9] A. El Shahat, A. Keyhani and H. El Shewy 400 kW Six Analytical High Speed Generator Designs for Smart Grid Systems // World Academy of Science, Engineering and Technology International Journal of Electrical, Computer, Energetic, Electronic and Communication Engineering Vol:4, №:3, 2010

[10] A. El Shahat, A. Keyhani and H. El Shewy Sizing a High Speed PM Generator for Green Energy Applications // JES 6–4 (2010): 501–516

[11] Adel El Shahat , Ali Keyhani Sizing High Speed Micro Generators for Smart Grid Systems // Smart Power Grids 2011, Part of the series Power Systems pp 177-234

[12] Binder, A. ; Schneider, T. Permanent magnet synchronous generators for regenerative energy conversion - a survey // Power Electronics and

Applications, 2005 European Conference on, 11-14 Sept. 2005, pp. 110

[13] Malmquist, A.; et al.: Mikrogasturbinen als Wegbereiter der dezentralen Wärme- und Stromversorgung, ABB Technik, 3/2000, p.22-30

[14] J. Saari, Thermal Analysis of High-Speed Induction Machines. Ph.D. Dissertation, Acta Polytechnica Scandinavica, 1998

[15] O. Aglen, A. Andersson, Thermal analysis of a high-speed generator, Industry Applications Conference, 2003. 38th IAS Annual Meeting. Conference Record of the, vol. 1, pp. 547–554, 12–16 Oct 2003

[16] Pierre-Daniel Pfister, Yves PerriardVery High Speed Slotless Permanent Magnet Motors: Analytical Modeling, Optimization, Design and Torque Measurement Methods // IEEE Transactions on industrial electronics, Vol. 57, №. 1, January 2010

[17] Aleksandar Borisavljevic Limits, Modeling and Design of High-Speed Permanent Magnet Machines // Printed by Wormann Print Service. – Zutphen, the Netherlands, 2011. – P. 209.

[18] Zhang Tao, Ye Xiaoting, Zhang Huiping, Jia Hongyun Strength Design on Permanent Magnet Rotor in High Speed Motor Using Finite Element Method // Telkomnika Indonesian Journal of Electrical Engineering. 2014.– vol.12. №3. pp. 1758–1763.

[19] 3. A.D. Boot, Бесконтактные электрические машины. Moscow, Russian Federation, 1990.

[20] 4. Ledovski A.N., Электрические машины с высококоэрцитивными постоянными магнитами . Moscow, Russian Federation, 1985 .

[21] Minos Beniakar. Themistoklis Kefalas, AntoniosKladasInvestigan of the Impact of the Operational Temperature of a Surface Permanent Magnet Motor // Materials Science Forum.– Vol. 670 (2011).– pp. 259–264

[22] F.R. Ismagilov, I.H. Khayrullin,V.E. Vavilov Model of transient thermal processes in contactless magnetoelectric machine. Electrical and data processing facilities and and systems (article in Russian with an abstract in English); 2013, № 3, 8-14.

[23] Sipaylov G.A., Salnikov D.I., Jadan V.A. Тепловые, гидравлические и аэродинамические расчеты в электрических машинах. Moscow, Russian Federation, 1989 .

[24] Filipov I.F. Основы теплообмена в электрических ашинах. Leningrad, Russian Federation, 1974.